
ANALOG-TO-STOCHASTIC CONVERTER USING MAGNETIC TUNNEL JUNCTION DEVICES FOR VISION CHIPS

A PREPRINT

Naoya Onizawa

Frontier Research Institute for Interdisciplinary Sciences, Tohoku University
 Sendai, Miyagi 980-8578, Japan
 nonizawa@m.tohoku.ac.jp

Daisaku Katagiri

Research Institute of Electrical Communication, Tohoku University
 Sendai, Miyagi 980-8577, Japan
 katagiri@ngc.riec.tohoku.ac.jp

Warren J. Gross

Department of Electrical and Computer Engineering, McGill University
 Montreal, Quebec H3A 0E9, Canada
 wjgross@mcgill.ca

Takahiro Hanyu

Research Institute of Electrical Communication, Tohoku University
 Sendai, Miyagi 980-8577, Japan
 hanyu@ngc.riec.tohoku.ac.jp

ABSTRACT

This paper introduces an analog-to-stochastic converter using a magnetic tunnel junction (MTJ) device for vision chips based on stochastic computation. Stochastic computation has been recently exploited for area-efficient hardware implementation, such as low-density parity-check (LDPC) decoders and image processors. However, power-and-area hungry two-step (analog-to-digital and digital-to-stochastic) converters are required for the analog to stochastic signal conversion. To realize a one-step conversion, an MTJ device is used as it inherently exhibits a probabilistic switching behavior between two resistance states. Exploiting the device-based probabilistic behavior, analog signals can be directly and area-efficiently converted to stochastic signals to mitigate the signal-conversion overhead. The analog-to-stochastic signal conversion is theoretically described and the conversion characteristic is evaluated using device and circuit parameters. In addition, the resistance variability of the MTJ device is considered in order to compensate the variability effect on the signal conversion. Based on the theoretical analysis, the analog-to-stochastic converter is designed in 90nm CMOS and 100nm MTJ technologies and is verified using a SPICE simulator (NS-SPICE) that handles both transistors and MTJ devices.

Keywords Stochastic computation, STT-MTJ, signal conversion, image sensor, feature extraction, cognitive system

1 Introduction

Stochastic computation [1, 2] has recently been exploited for area-efficient hardware implementation using probabilities represented by a random sequence of bits, called a *Bernoulli* sequence. Some applications of stochastic computation are low-density parity-check (LDPC) decoders [3–7] and image processors [8–10]. Stochastic computation

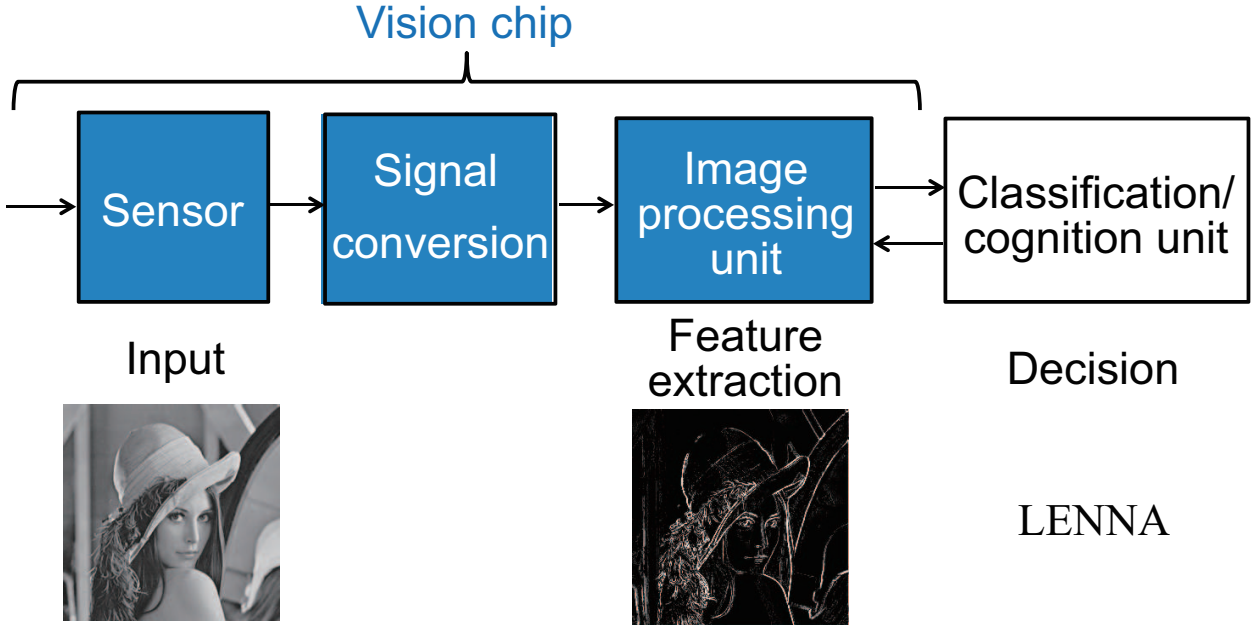


Figure 1: Example of a vision chip used in a cognitive system.

tends to be more error-tolerant than a conventional binary system as a bit-flip in stochastic computation corresponds to a least-significant-bit (LSB) error while a bit-flip on a most-significant-bit (MSB) error heavily affects a value in the conventional system [11].

The hardware based on stochastic computation is efficiently implemented, but an interface circuit to the stochastic hardware is required. In the stochastic image processors, analog signals from image sensors are converted to digital signals using analog-to-digital converters (ADC). Then, the digital signals are converted to stochastic bit streams using digital-to-signal converters that tend to be large because they consist of registers, linear-feedback shift registers (LFSRs), and comparators. To take advantage of the area efficiency on stochastic computation, the signal-conversion overhead needs to be mitigated. In [12], a concept of the analog-to-stochastic conversion has been proposed using memristors. However, the switching behavior of the memristor is very slow (the order of ms).

This paper introduces an analog-to-stochastic converter using a magnetic tunnel junction (MTJ) device for massively parallel vision chips. The vision chips are front-end image processors for feature extractions in cognitive computing as shown in Fig. 1. The MTJ device [13] is often exploited as a non-volatile memory that stores one-bit information as a resistance and is used for MRAMs and content-addressable memories [14, 15]. The MTJ device is at one of two resistance states and the switching speed between the two states is the order of ns. The switching behavior between the two states is probabilistic [16–18]. Exploiting the probabilistic behavior, analog signals are directly converted to stochastic bit streams in the proposed analog-to-stochastic converter. The signal conversion is theoretically described and is evaluated using device and circuit parameters to determine proper parameters for designing the analog-to-stochastic conversion.

The short version of this work was presented in [19], but it described only the theoretical analysis of the analog-to-stochastic converter. The extended work presented in this paper includes: (1) a more detailed theoretical analysis of the analog-to-stochastic converter by considering a voltage-bias effect, (2) considering a resistance variability of the MTJ device, (3) designing and simulating the analog-to-stochastic converter at the transistor level, and (4) simulating a simple vision chip including the proposed converter and a stochastic edge detector.

The rest of the paper is follows. Section II reviews the MTJ device and describes the probabilistic behavior. Section III describes the stochastic computation. Section IV introduces the analog-to-stochastic converter using the MTJ device and shows the circuit implementation. Section V describes a resistance-variability effect on the converter and a compensation technique of the variability. Section VI evaluates the signal-conversion characteristic using device and circuit parameters and verifies the signal conversion using a transistor-level simulator. Section VII concludes this paper.

2 Probabilistic Switching Behavior of MTJ Device

2.1 MTJ device

Fig. 2 (a) shows a perpendicular spin-transfer torque (STT) MTJ device [13] stacked on a CMOS layer [13]. The MTJ device consists of three main layers: a free layer, a tunnel-barrier layer, and a fixed layer, where there are a lot of additional layers in a real device. A spin direction is fixed in the fixed layer while it can be changed to one of two directions in the free layer. If the spin directions are the same in both layers, the MTJ device is on a parallel state that the MTJ resistance (R_{MTJ}) is low (R_P). Otherwise, it is on an anti-parallel state that R_{MTJ} is high (R_{AP}).

In the STT MTJ device, one-bit information is stored as a resistance using a current signal, I_w . Fig. 2 (b) shows a characteristic between R_{MTJ} and I_w . The anti-parallel state of the MTJ device is changed to the parallel state using I_w whose amount is $I_{AP \rightarrow P}$ during a specific period, such as several ns (see [13]). From the parallel to the anti-parallel state, the opposite direction of I_w is used, where the amount of current is $I_{P \rightarrow AP}$.

2.2 Switching probability

The switching behavior of the MTJ device is probabilistic in [16–18]. In several literatures, the probabilistic behaviour is exploited for MRAMs, synapse systems, and random number generators [20–22]. Fig. 3 shows a probabilistic behavior of the MTJ device. Suppose that the initial state of the MTJ device is parallel. When one-bit information is written in the MTJ device, a write current signal, I_w , is applied during a specific period of t . The switching probability of the MTJ device, p_w , is defined as follows [16]:

$$p_w = 1 - \exp(-t/\tau_p), \quad (1)$$

where τ_p is the switching time constant. Eq. (1) is based on [23] whose model derives from [24]. τ_p is calculated on either regions I or II described as follows.

To calculate p_w , a critical current, I_c , needs to be defined. I_c is differently defined in two regions: region I ($\tau_p \gg \tau_0$) and region II ($\tau_p < \text{several tens times } \tau_0$), where τ_0 is the attempt time for thermal switching (around 1 ns) (see [16]). In the region I (thermal activation region), the state of the MTJ device is mainly changed based on a thermal effect. The thermal effect is expressed as $\ln(\tau_p/\tau_0) = (E/k_B T)$, where E is the actual magnetic anisotropy energy of a magnetic cell, k_B is the Boltzmann constant, and T is the absolute temperature. I_c is defined as follows:

$$I_c = I_{c0t}(1 - (k_B T/E) \ln(\tau_p/\tau_0)), \quad (2)$$

where I_{c0t} is the extrapolated I_c at $\tau_p = \tau_0$. In the region II, the state of the MTJ device is mainly changed by a spin-injection effect. I_c is defined as follows:

$$I_c = I_{c0s} \left(1 + \frac{\tau_{relax}}{\tau_p} \ln \left(\frac{\pi/2}{\sqrt{k_B T/E}} \right) \right), \quad (3)$$

where I_{c0s} is the extrapolated I_c at $\tau_p \sim \infty$ and τ_{relax} is the relaxation time of a magnetic moment. Using the probabilistic behavior, an analog-to-stochastic converter is designed for image processors based on stochastic computation.

3 Stochastic computation

Stochastic computation was first introduced in 1960s [1] and has recently been exploited for some applications [2], such as LDPC decoding [3–7] and image processing [8–10]. Stochastic computation performs in probabilistic domain that the probability is represented by a random sequence of bits, called a *Bernoulli* sequence. The probability is determined by the frequency of ones or zeros in the sequence that can be represented by many different sequences of bits. For example, different sequences of bits (1010) and (0011) mean the same probability.

The advantage of stochastic computation is low-cost hardware implementation. Fig. 4 shows a multiplier based on stochastic computation. Let $p(A) = \Pr(A=1)$ and $p(B) = \Pr(B=1)$ be the probabilities represented by the two input bit streams and $p(C) = \Pr(C=1)$ be the probability represented by the output bit stream. The multiplication is described as $p(C) = p(A) * p(B)$ that is simply designed using a 2-input AND gate, where the computation performs bit-serially. Hence, this technique results in efficient hardware implementations for algorithms that compute with probabilities such as LDPC decoders.

In contrast, the disadvantage of stochastic computation is a signal conversion. Fig. 5 (a) shows a conventional analog-to-stochastic converter for stochastic computation. For example, in image processing, an analog signal is received

from a sensor and is then converted to a digital signal using an analog-to-digital converter (ADC). The digital signal is stored in registers and is then compared with random bits that typically generated using a linear feedback shift register (LFSR) to convert to a stochastic signal. The relationship among the three signals is summarized in Fig. 6 (a).

The power dissipation of the ADC is a large portion of the total power dissipation in an image sensor (e.g. 65% in [25]). In addition, the digital-to-stochastic converter tends to be large in the stochastic circuits. To estimate the overhead, an edge-detection circuit based on stochastic computation [8] is designed using Verilog-HDL and is synthesized using Synopsys Design Compiler on Silterra 0.13 μm CMOS technology. The synthesized result shows that the area of the digital-to-stochastic converter is 43.6% of the total area when the bit width of the LFSRs is 10 bits.

To reduce the overhead of the signal conversion, an analog-to-stochastic converter is presented that the analog signal is directly converted to the stochastic signal as shown in Fig. 5 (b).

4 Analog-to-Stochastic Conversion Using MTJ Device

4.1 Overall structure

Fig. 7 shows the proposed analog-to-stochastic converter using the MTJ device. Suppose that an analog current signal is received in a logarithm image sensor that realizes a high dynamic range [26–28]. The analog voltage signal is the output of the image sensor and is the input of the analog-to-stochastic converter. The analog-to-stochastic converter is designed using three transistors and one MTJ device. The output of the converter connects to a latch that stores a stochastic bit generated.

Fig. 8 shows the circuit operation of the proposed analog-to-stochastic converter. The converter operates at one of three phases: write, set, and erase. After the end of the erase phase, the phase is back to the write phase.

4.2 Write phase

In the write phase, the analog input current signal, I_{ph} , is converted to the analog output voltage signal, V_{ph} , as follows:

$$V_{ph} = V_{dd} - n \frac{k_B T}{q} \ln\left(\frac{I_{ph}}{I_{d0}}\right), \quad (4)$$

where n is 1.3 - 2, I_{d0} is the process dependent parameter and q is the elementary charge [27]. Then, V_{ph} is applied to the analog-to-stochastic converter to generate a write current signal, I_w , defined as follows:

$$I_w = \frac{V_{dd} - V_{bias}}{R_{MTJ}} - n \frac{k_B T}{q R_{MTJ}} \ln\left(\frac{I_{ph}}{I_{d0}}\right), \quad (5)$$

where V_{bias} is the bias voltage to control I_w .

The resistance, R_{MTJ} , varies depending on a bias voltage to the MTJ device, $V_b (=V_{ph}-V_{bias})$ when a current flows through the MTJ device [13]. Especially, the resistance at the anti-parallel state is more sensitive to the bias voltage than that at the parallel state. To mitigate the bias-voltage effect, the parallel state is used as the initial state of the MTJ device in the converter. The resistance at the parallel state with the bias voltage effect is defined as R_{Pb} that is described as:

$$R_{Pb} = R_P (1 + BC1|V_b| + BC2|V_b|^2), \quad (6)$$

where BC1 and BC2 are the first and second-bias coefficients, respectively. R_P is the resistance at the parallel state when the bias voltage is 0. I_w is redefined as

$$I_w = \frac{V_{dd} - V_{bias}}{R_{Pb}} - n \frac{k_B T}{q R_{Pb}} \ln\left(\frac{I_{ph}}{I_{d0}}\right). \quad (7)$$

Suppose that the switching characteristic of the MTJ device is determined by the region II described in equation (3). The switching time constant, τ_p , is defined as follows:

$$\tau_p = \frac{I_{c0s} \tau_{relax} \ln \frac{\pi/2}{\sqrt{k_B T/E}}}{I_w - I_{c0s}}. \quad (8)$$

A non-switching probability, $\overline{p_w}$, is defined as $1 - p_w$, where p_w is described in equation (1). The non-switching probability in logarithm domain, $\ln \overline{p_w}$, is described as follows:

$$\ln \overline{p_w} = -t/\tau_p. \quad (9)$$

Using equations (8) and (9), $\ln \overline{p_w}$ is defined as follows:

$$\ln \overline{p_w} = -\alpha(I_w - I_{c0s}), \quad (10)$$

where α is $t/\left(I_{c0s} t_{relax} \ln\left(\frac{\pi/2}{\sqrt{k_B T/E}}\right)\right)$. Using equations (7) and (10), $\ln \overline{p_w}$ is redefined as follows:

$$\ln \overline{p_w} = \beta \ln\left(\frac{I_{ph}}{I_{d0}}\right) + \alpha\left(I_{c0s} - \frac{(V_{dd} - V_{bias})}{R_{Pb}}\right), \quad (11)$$

where $\beta = \alpha n \frac{k_B T}{q R_{Pb}}$. β has to be equal to 1 to ensure a linear relationship between the analog input signal, I_{ph} , and the probability of the stochastic bit stream, p_w . The linear relationship is required for the analog-to-stochastic converter. From this, one derives α as follows:

$$\alpha = \frac{q R_{Pb}}{n k_B T}, \quad (12)$$

and thus the pulse duration, t , is given by:

$$t = \left(I_{c0s} t_{relax} \ln\left(\frac{\pi/2}{\sqrt{k_B T/E}}\right)\right) \cdot \frac{q R_{Pb}}{n k_B T}. \quad (13)$$

4.3 Set and erase phases

Once one-bit information is stored in the MTJ device at p_w , the converter operates at the set phase shown in Fig. 8 (b). At the set phase, V_{set} is high and hence the voltage signal, V_R , is determined by the MTJ state defined as follows:

$$V_R = \begin{cases} \text{High ("1")} & \text{if } R_{MTJ} = R_P \\ \text{Low ("0")} & \text{otherwise} \end{cases} \quad (14)$$

Then, V_R is stored in the latch next to the converter as shown in Fig. 7.

After outputting the stochastic bit, the converter operates at the erase phase shown in Fig. 8 (c). At the erase phase, the erase current, I_e , is applied to change R_{MTJ} back to R_P , where the current direction of I_e , is opposite to that of I_w . Finally, the operation phase returns to the write phase to generate a new stochastic bit.

5 Consideration of MTJ Variability

5.1 Theoretical analysis

In this section, a resistance variability of an MTJ device is considered. In the analog-to-stochastic converter, the resistance variability affects the write current in equation (7), and hence the switching probability in equation (11). In this case, an analog input signal is not properly converted to a stochastic bit stream in the converter.

Here, the resistance variability is defined by ΔR . The write current considering the resistance variability, I'_w , is defined using equation (7) as follows:

$$I'_w \simeq \frac{V_{dd} - V'_{bias}}{(R_{Pb} + \Delta R)} - n \frac{k_B T}{q(R_{Pb} + \Delta R)} \ln\left(\frac{I_{ph}}{I_{d0}}\right), \quad (15)$$

where V'_{bias} is an updated parameter of V_{bias} in case of considering the MTJ variability. Suppose that R_{Pb} defined in equation (6) is not affected by changing V_{bias} to V'_{bias} .

In addition, the switching probability considering the MTJ variability, p'_w , is defined using equation (11) as follows:

$$\ln \overline{p'_w} \simeq \beta' \ln\left(\frac{I_{ph}}{I_{d0}}\right) + \alpha'\left(I_{c0s} - \frac{(V_{dd} - V'_{bias})}{(R_{Pb} + \Delta R)}\right), \quad (16)$$

where α' and β' are updated parameters of α and β , respectively, in case of considering the MTJ variability. As shown in the two equations, the write current and the switching probability are affected by ΔR . To compensate the ΔR effect, three parameters, such as α' , β' , and V_{bias} are controlled.

First, let us consider β' in equation (16). As β is $\alpha n \frac{k_B T}{q R_{Pb}}$, β' is defined as follows:

$$\beta' \simeq \frac{t'}{\left(I_{c0s} t_{relax} \ln\left(\frac{\pi/2}{\sqrt{k_B T/E}}\right)\right)} \cdot \frac{n k_B T}{q(R_{Pb} + \Delta R)}, \quad (17)$$

where t' is an updated parameter of t in case of considering the resistance variability. In equation (17), there is a variable parameter, t' , to compensate the resistance variability. To realize the linear relationship between the analog input signal, I_{ph} , and the probability of the stochastic bit stream, p_w under the resistance variability, β' has to be 1. Hence, the resistance variability in terms of β' is compensated by the write attempt time, t' , as follows:

$$t' \simeq \left(I_{c0s} t_{relax} \ln \left(\frac{\pi/2}{\sqrt{k_B T/E}} \right) \right) \cdot \frac{q(R_{Pb} + \Delta R)}{nk_B T}. \quad (18)$$

Using equations (13) and (18), t' is redefined as follows:

$$t' \simeq t \left(1 + \frac{\Delta R}{R_{Pb}} \right). \quad (19)$$

When β' is equal to 1, α' based on equation (12) is given by:

$$\alpha' \simeq \frac{q(R_{Pb} + \Delta R)}{nk_B T}. \quad (20)$$

Next, let us consider α' and $\frac{(V_{dd} - V'_{bias})}{(R_{Pb} + \Delta R)}$ in equation (16). To maintain the same switching probability under the resistance variability, we need to satisfy an equation using equations (11) and (16) as follows:

$$\alpha \left(I_{c0s} - \frac{(V_{dd} - V_{bias})}{R_{Pb}} \right) \simeq \alpha' \left(I_{c0s} - \frac{(V_{dd} - V'_{bias})}{(R_{Pb} + \Delta R)} \right) \quad (21)$$

Using (12), (20), and (21), V'_{bias} is defined as follows:

$$V'_{bias} \simeq V_{bias} - \Delta R I_{c0s}. \quad (22)$$

Based on the theoretical analysis, we can control t' and V_{bias} to maintain the same switching probability under the resistance variability.

5.2 Compensation of resistance variability

Fig. 9 shows a block diagram of the proposed analog-to-stochastic converter considering the resistance variability. It consists of a pulse-signal generator, a random bit generator, a counter, and a probability controller. Suppose that the two parameters, t' and V'_{bias} , are set as a calibration step before using the converter.

First, an input-voltage signal, V_{ph} , is tested using default parameters of t and V_{bias} to generate a stochastic bit stream whose probability is 50%. Then, the number of 1's in the bit stream is counted and the probability is checked in the probability controller. If the probability is not 50%, then V'_{bias} is controlled. For example, if the probability is less than 50%, the MTJ resistance is larger than that without variability.

Once a probability of 50% is obtained, different input-voltage signals are tested to generate different probabilities. If the relationship between the analog input signal and the probability is not linear, t' is controlled to set $\beta' = 1$. After setting the two parameters desired, the analog-to-stochastic converter is ready to start.

6 Evaluation

6.1 Theoretical analysis

The proposed analog-to-stochastic converter is evaluated using device and circuit parameters shown in Table 1. Parameters, I_{d0} and n , in image sensors are derived from [27] and device parameters, such as I_{c0s} , R_P , R_{AP} , $E/k_B T$, and t_{relax} , are derived from [13, 16]. The circuit parameters are based on ASPLA 90nm CMOS technology and the MTJ-device parameters are based on a 100nm MTJ technology.

Fig. 10 shows a relationship between the write current at the MTJ device, I_w , and the analog input current, I_{ph} , based on equation (7). In equation (7), I_{ph} is only a variable. The other parameters, except V_{bias} are device dependent and constant. V_{bias} are used to control the amount of I_w .

Fig. 11 shows a relationship between the inverse of the switching time constant, τ_p , and I_w based on equation (8) when V_{bias} is 0.4 V. When the critical current, I_{c0s} , is decreased, τ_p is decreased. It means that the MTJ device is more easily switched to another state using the same amount of current, I_w , when I_{c0s} is smaller. I_{c0s} is decreased when the MTJ technology is advanced [29], reducing the write energy and the write attempt time, t .

Table 1: Device and circuit parameters.

Parameters	Name	Value
V_{dd}	Supply voltage	1.2 V
I_{d0}	-	0.1 nA
n	-	2
T	Absolute temperature	300 K
I_{c0s}	Critical current	50 μ A to 200 μ A
R_P	Resistance (P)	1 k Ω
R_{AP}	Resistance (AP)	3 k Ω
$E/k_B T$	-	60
t_{relax}	Relaxation time	500 ps
t	Attempt time of I_w	1 - 10 ns
V_{bias}	Bias voltage	0 - 0.4 V

Fig. 12 shows a relationship between the non-switching probability of the MTJ device, \bar{p}_w , and I_{ph} , when V_{bias} is 0.4 V and I_{c0s} is 200 μ A based on equation (11). The attempt time, t , varies from 1 to 10 ns. When I_{ph} is increased, I_w is decreased, reducing p_w . Depending on t , the parameter, β , in equation (11) is changed, affecting the slope in Fig. 12. When β is set to 1 by choosing $t = 4.73$ ns, the relationship between p_w and I_{ph} is linear, realizing the analog-to-stochastic conversion.

6.2 Theoretical analysis with considering MTJ variability

Fig. 13 shows a relationship between \bar{p}'_w and I_{ph} under the resistance variability of the MTJ device, where V'_{bias} is 0.4 V, I_{c0s} is 200 μ A and t is 4.73 ns. The relationship is given by equation (16). A resistance variability of 10 % at most is considered. Compared with the relationship without the variability, the switching probabilities considering the variability are different.

To compensate the variability, only V'_{bias} is controlled as shown in Fig. 14. V'_{bias} are determined based on equation (22). After setting V'_{bias} , the switching probabilities are close to that without the resistance variability. However, the linear relationships between the switching probabilities and the analog input current signal are not obtained.

To control both V_{bias}' and t' , the relationships between the switching probabilities and the analog input current signal are almost linear under the resistance variability as shown in Fig. 15. t' are determined based on equation (19).

6.3 Simulation results

To verify the circuit operation of the proposed analog-to-stochastic converter, the proposed converter is designed using device and circuit parameters used in Fig. 12. Fig. 16 shows simulated waveforms of the proposed analog-to-stochastic converter. It is simulated using NS-SPICE [23] in 90nm CMOS and 100nm MTJ technologies. NS-SPICE is a transistor-level simulator that can handle both the transistors and the MTJ devices. The cycle time of the converter is set to 10 ns, where the write phase is 5 ns, and the set phase is 1 ns, and the erase phase is 4 ns. At the write phase, there is a write current during 4.73 ns and no current during 0.27 ns. The write current, I_w , is 236 μ A corresponding to the switching probability, p_w , of 50%.

In this simulation, the proposed converter generates three stochastic bits. Note that the resistance of the MTJ device is not the same as R_P or R_{AP} because of the bias voltage effect. At the first and the second trials, the resistance of the MTJ device is changed from the parallel to the anti-parallel state at the write phase. Hence, the output of the converter, V_{OUT} is “0”. In contrast, at the third trial, the resistance of the MTJ device is not changed even if I_w is applied to the MTJ device. In this case, V_{OUT} is “1”.

Fig. 17 shows a monte-carlo simulation of the proposed analog-to-stochastic converter at the write phase. The number of trials is 100 and I_w is 236 μ A corresponding to p_w of 50%. The simulation waveforms show that the switching behavior of the MTJ device is probabilistic and the switching timing is random. In this simulation, the resistance of the MTJ device is changed to R_{AP} of 3 k Ω at 50% after writing a bit to the MTJ device.

6.4 Design example of a vision chip for cognitive systems

Fig. 18 shows a simulation model of a simple vision including an error-injection module. Suppose the simple vision chip receives analog input signals of an image from a sensor and extracts the feature of the image for cognitive systems.

The feature extraction unit is designed using a stochastic edge detector [8, 9]. The simulation model is designed and evaluated using MATLAB, where the analog-to-stochastic converter is simply modelled as a random bit generator. It is because the precise model of the MTJ device requires transistor-level modelling. It is also possible to include NS-SPICE in MATLAB to emulate the switching behavior of the MTJ device in [30]. The simulation model also includes an error injection module that models wrong bits that might be generated in the analog-to-stochastic converter.

Fig. 19 (a) shows stochastic edge-detection results based on Fig. 18 under input soft errors. A standard grayscale test image, LENNA, is used to evaluate the error effects. The number of stochastic bits is set to 1,000. The simulated images show that the image qualities are not strongly affected by input errors, because stochastic computation is highly robust against soft errors. In contrast, the conventional binary implementation heavily suffers from soft errors as shown in Fig. 19 (b). As a result, the stochastic edge-detection result would be useful for cognitive systems, even if the proposed converter generates wrong stochastic bits at a small error rate.

7 Conclusion

In this paper, the analog-to-stochastic converter using MTJ devices has been proposed for the stochastic computation based vision chips. Thanks to the probabilistic behavior of MTJ devices, analog signals from image sensors are directly and area-efficiently converted to stochastic bit streams without power-and-area hungry analog-to-digital and digital-to-stochastic converters. The MTJ based analog-to-stochastic conversion is theoretically described and is evaluated using device and circuit parameters. As a result, a linear relationship between the analog signal and the probability of stochastic bit stream is realized by setting a specific attempt time of the write current. In addition, the resistance variability of the MTJ device is theoretically analyzed. It shows that the variability can be compensated by controlling the attempt time of writing and a bias voltage at a calibration step before using the converter. Based on the theoretical analysis, the analog-to-stochastic converter is designed using in 90nm CMOS and 100nm MTJ technologies. The proposed converter simulated using NS-SPICE generates a stochastic bit stream. In addition, the simple vision chip including an analog-to-stochastic converter and a stochastic edge detector is designed and simulated in MATLAB for future cognitive systems.

Future work includes a more detailed circuit implementation of the proposed converter including the calibration block for fabrication. It also includes designing a whole cognitive system including the stochastic vision chip based on the analog-to-stochastic converter.

Acknowledgment

This work was supported by JSPS KAKENHI Grant Number 26700003 and MEXT Brainware LSI Project. This work is supported by VLSI Design and Education Center (VDEC), The University of Tokyo with the collaboration with Synopsys Corporation.

References

- [1] B. R. Gaines, “Stochastic computing systems,” *Adv. Inf. Syst. Sci. Plenum*, vol. 2, no. 2, pp. 37–172, 1969.
- [2] B. Brown and H. Card, “Stochastic neural computation. i. computational elements,” *IEEE Transactions on Computers*, vol. 50, no. 9, pp. 891–905, Sep 2001.
- [3] V. Gaudet and A. Rapley, “Iterative decoding using stochastic computation,” *Electronics Letters*, vol. 39, no. 3, pp. 299 – 301, Feb. 2003.
- [4] S. Sharifi Tehrani, W. Gross, and S. Mannor, “Stochastic decoding of LDPC codes,” *IEEE Communications Letters*, vol. 10, no. 10, pp. 716 –718, Oct. 2006.
- [5] S. Sharifi Tehrani, S. Mannor, and W. Gross, “Fully parallel stochastic LDPC decoders,” *IEEE Transactions on Signal Processing*, vol. 56, no. 11, pp. 5692 –5703, Nov. 2008.
- [6] S. Sharifi Tehrani, A. Naderi, G.-A. Kamendje, S. Hemati, S. Mannor, and W. Gross, “Majority-based tracking forecast memories for stochastic LDPC decoding,” *IEEE Transactions on Signal Processing*, vol. 58, no. 9, pp. 4883 –4896, Sep. 2010.
- [7] N. Onizawa, W. Gross, T. Hanyu, and V. Gaudet, “Clockless stochastic decoding of low-density parity-check codes: Architecture and simulation model,” *Journal of Signal Processing*, Sep. 2013.
- [8] P. Li and D. Lilja, “Using stochastic computing to implement digital image processing algorithms,” in *2011 IEEE 29th International Conference on Computer Design (ICCD)*, Oct 2011, pp. 154–161.

[9] P. Li, D. Lilja, W. Qian, K. Bazargan, and M. Riedel, “Computation on stochastic bit streams digital image processing case studies,” *IEEE Transactions on Very Large Scale Integration (VLSI) Systems*, vol. 22, no. 3, pp. 449–462, March 2014.

[10] N. Onizawa, D. Katagiri, K. Matsumiya, W. Gross, and T. Hanyu, “Gabor filter based on stochastic computation,” *IEEE Signal Processing Letters*, vol. 22, no. 9, pp. 1224–1228, Sept 2015.

[11] W. Qian, X. Li, M. Riedel, K. Bazargan, and D. Lilja, “An architecture for fault-tolerant computation with stochastic logic,” *IEEE Transactions on Computers*, vol. 60, no. 1, pp. 93–105, Jan 2011.

[12] P. Knag, W. Lu, and Z. Zhang, “A native stochastic computing architecture enabled by memristors,” *IEEE Transactions on Nanotechnology*, vol. 13, no. 2, pp. 283–293, March 2014.

[13] S. Ikeda et al., “A perpendicular-anisotropy CoFeB–MgO magnetic tunnel junction,” *Nature Materials*, vol. 9, pp. 721 – 724, 2010.

[14] T. Kawahara, R. Takemura, K. Miura, J. Hayakawa, S. Ikeda, Y. M. Lee, R. Sasaki, Y. Goto, K. Ito, T. Meguro, F. Matsukura, H. Takahashi, H. Matsuoka, and H. Ohno, “2 Mb SPRAM (spin-transfer torque ram) with bit-by-bit bi-directional current write and parallelizing-direction current read,” *IEEE Journal of Solid-State Circuits*, vol. 43, no. 1, pp. 109–120, Jan 2008.

[15] S. Matsunaga et al., “Fabrication of a 99%-energy-less nonvolatile multi-functional CAM chip using hierarchical power gating for a massively-parallel full-text-search engine,” in *2013 Symposium on VLSI Circuits (VLSIC)*, June 2013, pp. C106–C107.

[16] K. Yagami, A. Tulapurkar, A. Fukushima, and Y. Suzuki, “Inspection of intrinsic critical currents for spin-transfer magnetization switching,” *IEEE Transactions on Magnetics*, vol. 41, no. 10, pp. 2615–2617, Oct 2005.

[17] Z. Diao, Z. Li, S. Wang, Y. Ding, A. Panchula, E. Chen, L.-C. Wang, and Y. Huai, “Spin-transfer torque switching in magnetic tunnel junctions and spin-transfer torque random access memory,” *Journal of Physics: Condensed Matter*, vol. 19, no. 16, p. 165209, 2007. [Online]. Available: <http://stacks.iop.org/0953-8984/19/i=16/a=165209>

[18] H. Zhao, Y. Zhang, P. Amiri, J. Katine, J. Langer, H. Jiang, I. Krivorotov, K. Wang, and J.-P. Wang, “Spin-torque driven switching probability density function asymmetry,” *IEEE Transactions on Magnetics*, vol. 48, no. 11, pp. 3818–3820, Nov 2012.

[19] N. Onizawa, D. Katagiri, W. Gross, and T. Hanyu, “Analog-to-stochastic converter using magnetic-tunnel junction devices,” in *2014 IEEE/ACM International Symposium on Nanoscale Architectures (NANOARCH)*, July 2014, pp. 59–64.

[20] Y. Zhang, W. Zhao, J.-O. Klein, W. Kang, D. Querlioz, C. Chappert, and D. Ravelosona, “Multi-level cell spin transfer torque MRAM based on stochastic switching,” in *2013 13th IEEE Conference on Nanotechnology (IEEE-NANO)*, Aug 2013, pp. 233–236.

[21] A. Vincent, J. Larroque, W. Zhao, N. Ben Romdhane, O. Bichler, C. Gamrat, J.-O. Klein, S. Galdin-Retailleau, and D. Querlioz, “Spin-transfer torque magnetic memory as a stochastic memristive synapse,” in *2014 IEEE International Symposium on Circuits and Systems (ISCAS)*, June 2014, pp. 1074–1077.

[22] A. Fukushima, T. Seki, K. Yakushiji, H. Kubota, H. Imamura, S. Yuasa, and K. Ando, “Spin dice: A scalable truly random number generator based on spintronics,” *Applied Physics Express*, vol. 7, no. 8, p. 083001, 2014. [Online]. Available: <http://stacks.iop.org/1882-0786/7/i=8/a=083001>

[23] N. Sakimura, R. Nebashi, Y. Tsuji, H. Honjo, T. Sugibayashi, H. Koike, T. Ohsawa, S. Fukami, T. Hanyu, H. Ohno, and T. Endoh, “High-speed simulator including accurate mtj models for spintronics integrated circuit design,” in *2012 IEEE International Symposium on Circuits and Systems (ISCAS)*, May 2012, pp. 1971–1974.

[24] N. D. Rizzo, M. DeHerrera, J. Janesky, B. Engel, J. Slaughter, and S. Tehrani, “Thermally activated magnetization reversal in submicron magnetic tunnel junctions for magnetoresistive random access memory,” *Applied Physics Letters*, vol. 80, no. 13, 2002.

[25] Y. Oike and A. El Gamal, “CMOS image sensor with per-column $\Sigma\Delta$ ADC and programmable compressed sensing,” *IEEE Journal of Solid-State Circuits*, vol. 48, no. 1, pp. 318–328, Jan 2013.

[26] D. Stoppa, A. Simoni, L. Gonzo, M. Gottardi, and G.-F. Dalla Betta, “Novel CMOS image sensor with a 132-dB dynamic range,” *IEEE Journal of Solid-State Circuits*, vol. 37, no. 12, pp. 1846–1852, Dec 2002.

[27] H. Amhaz, H. Zimouche, and G. Sicard, “Smart readout technique designed for logarithmic CMOS image sensor including a motion detection scheme,” in *2011 IEEE 9th International New Circuits and Systems Conference (NEWCAS)*, June 2011, pp. 49–52.

[28] W.-F. Chou, S.-F. Yeh, C.-F. Chiu, and C.-C. Hsieh, “A linear-logarithmic CMOS image sensor with pixel-FPN reduction and tunable response curve,” *IEEE Sensors Journal*, vol. 14, no. 5, pp. 1625–1632, May 2014.

- [29] H. Sato, T. Yamamoto, M. Yamanouchi, S. Ikeda, S. Fukami, K. Kinoshita, F. Matsukura, N. Kasai, and H. Ohno, “Comprehensive study of CoFeB-MgO magnetic tunnel junction characteristics with single- and double-interface scaling down to 1X nm,” in *2013 IEEE International Electron Devices Meeting (IEDM)*, Dec 2013, pp. 3.2.1–3.2.4.
- [30] S. Oosawa, T. Konishi, N. Onizawa, and T. Hanyu, “Design of an STT-MTJ based true random number generator using digitally controlled probability-locked loop,” in *13th IEEE New Circuits and Systems (NEWCAS)*, June 2015, pp. 1–4.

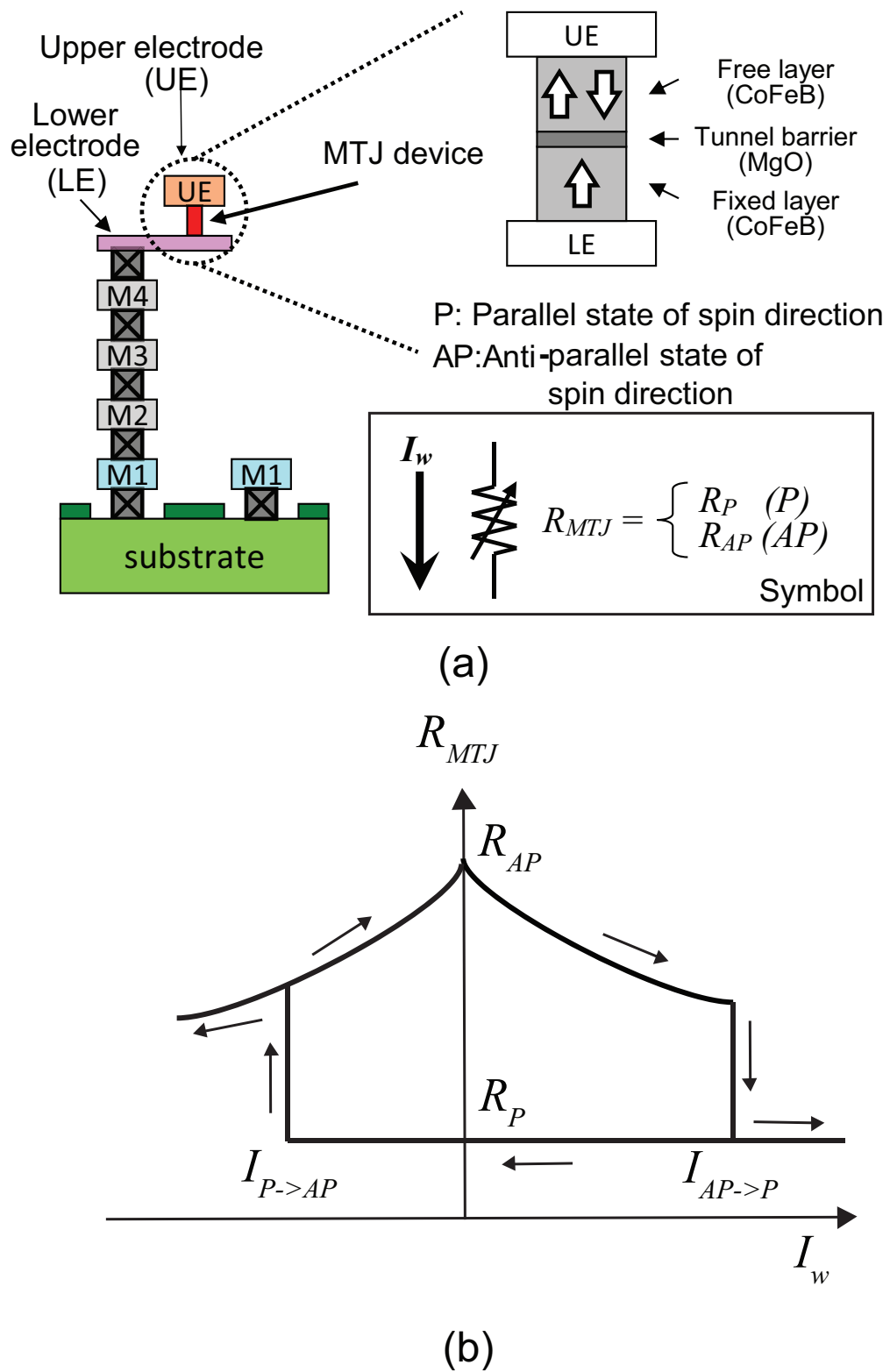


Figure 2: Spin-transfer torque (STT) MTJ device: (a) stacked on a CMOS layer and (b) its R-I characteristic.

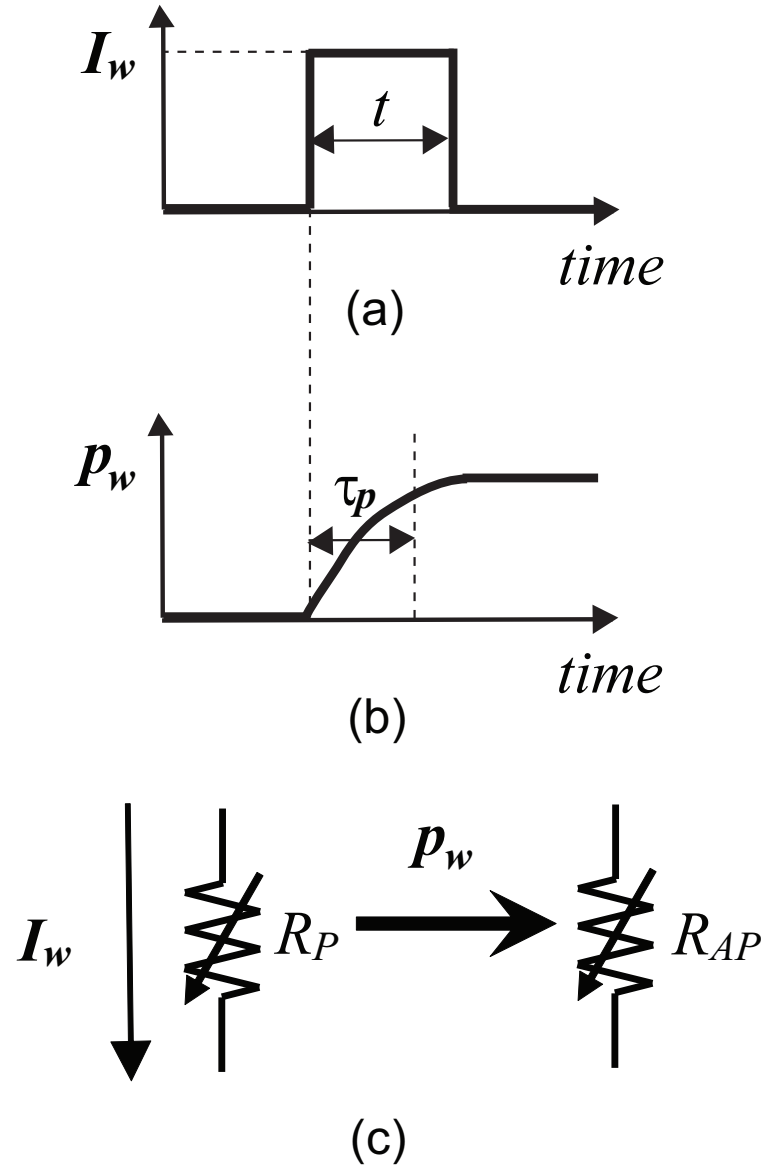


Figure 3: Probabilistic behavior of MTJ device: (a) write current (I_w), (b) switching probability (p_w), and (c) switching behavior. The MTJ state is probabilistically changed to another state.

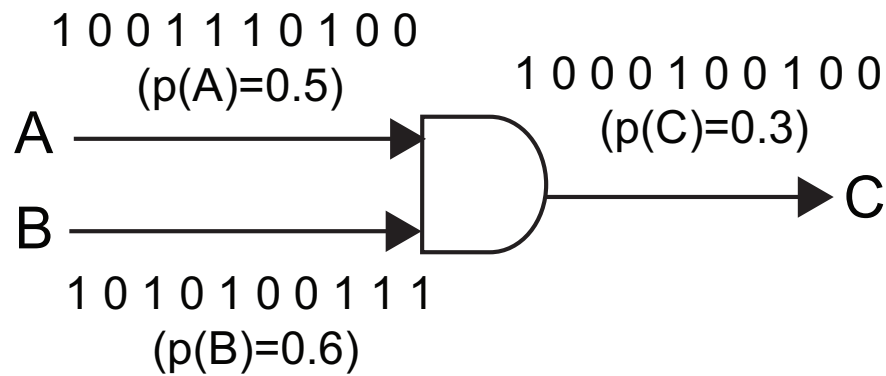
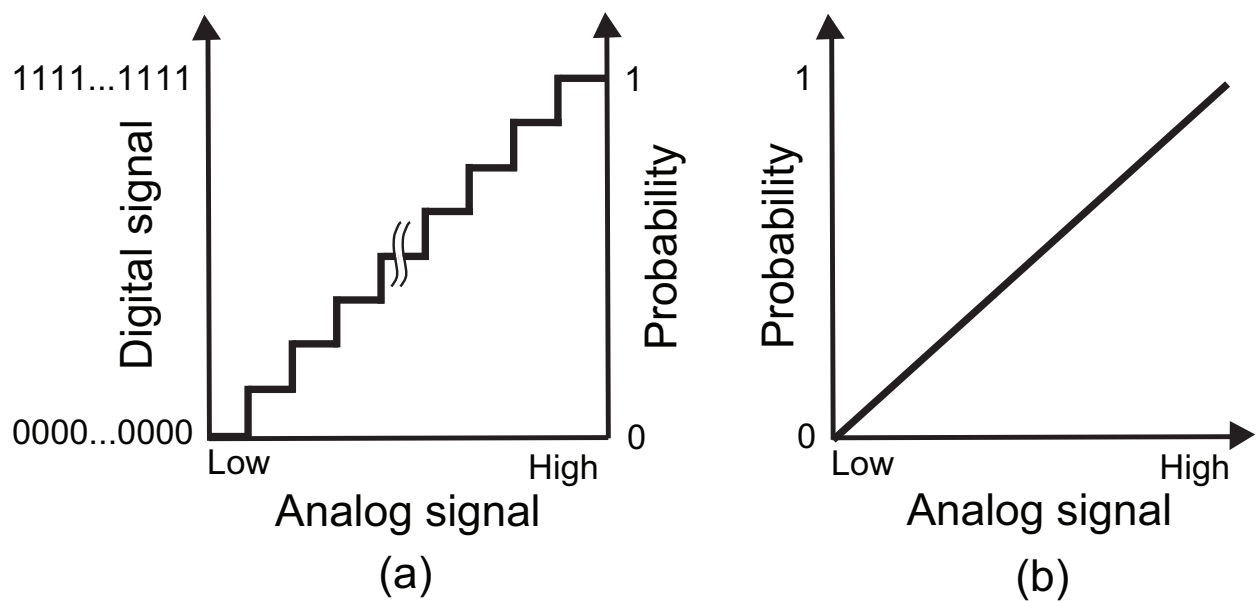
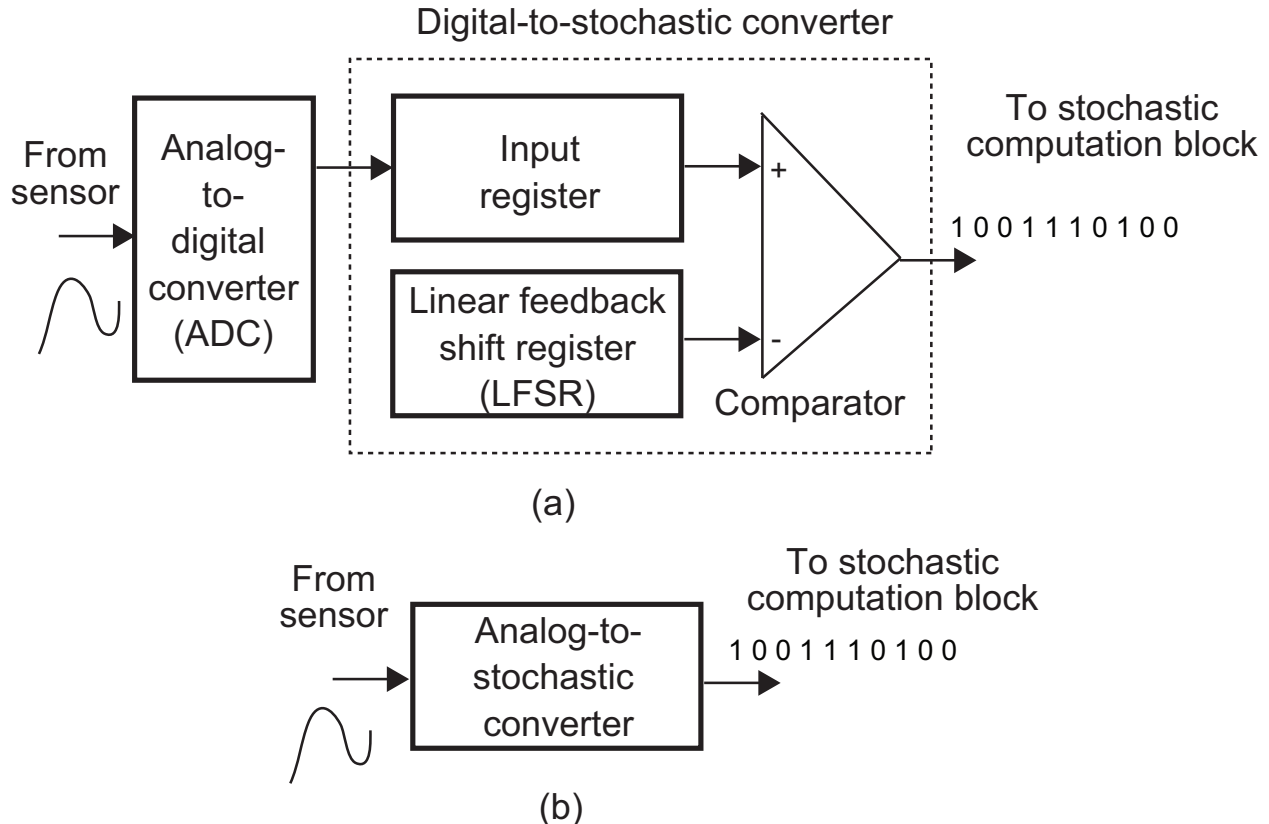


Figure 4: Multiplier based on stochastic computation designed using a 2-input AND gate.



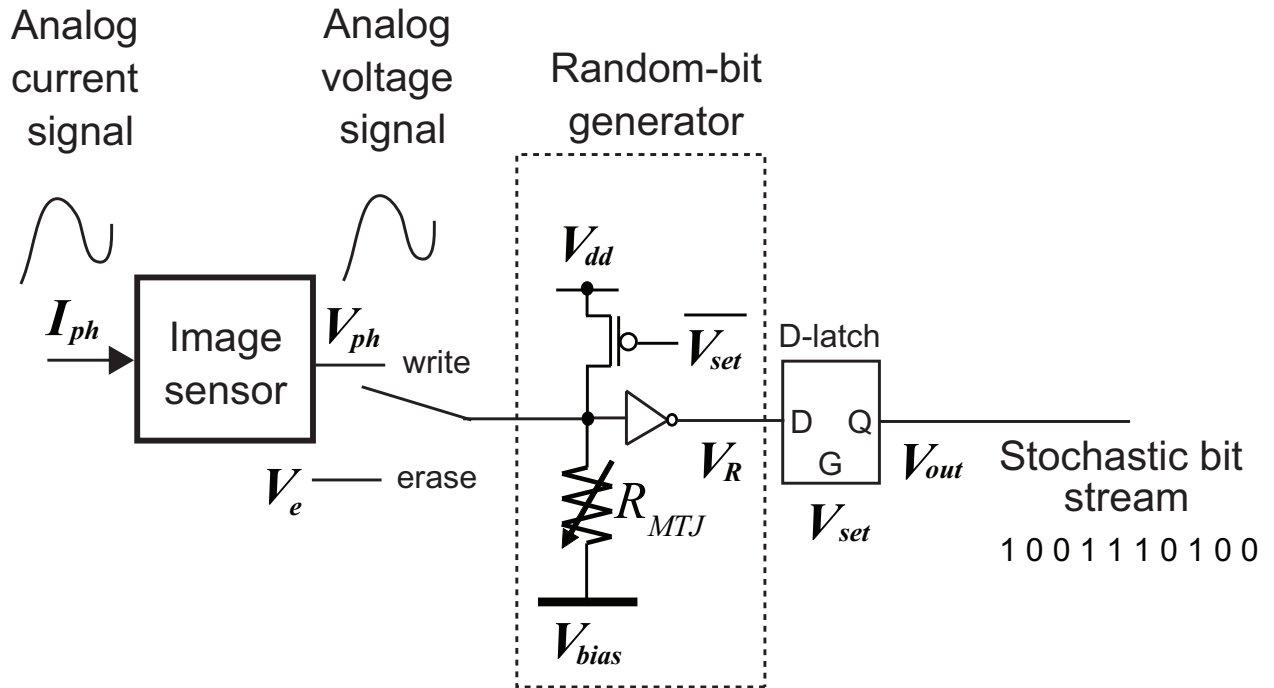
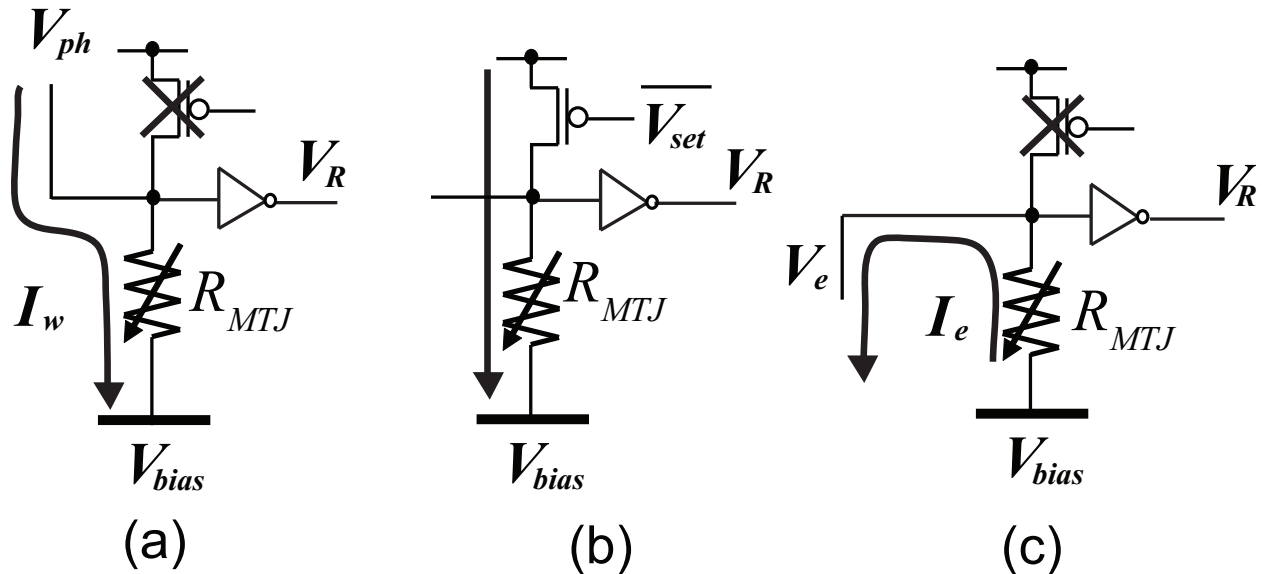


Figure 7: Overall structure of the proposed analog-to-stochastic converter.

Figure 8: Circuit of the analog-to-stochastic converter that operates at one of : (a) write, (b) set, and (c) erase phases. One-bit information is stored at p_w in the write phase and the stored MTJ state is set to the output in the set phase and finally the MTJ state is erased in the erase phase.

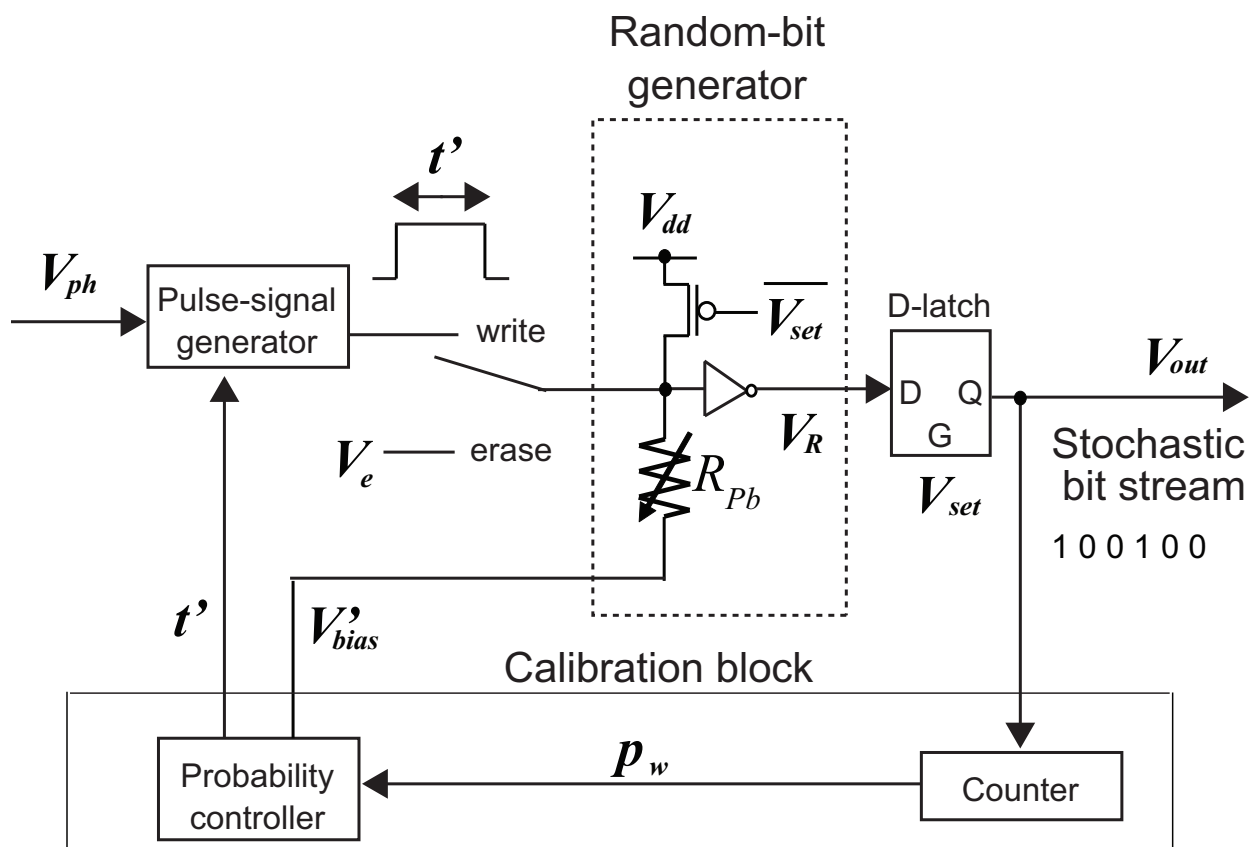


Figure 9: Overall structure of the proposed analog-to-stochastic converter considering a resistance variability of the MTJ device. t' and V'_{bias} are controlled to compensate the variability as a calibration step.

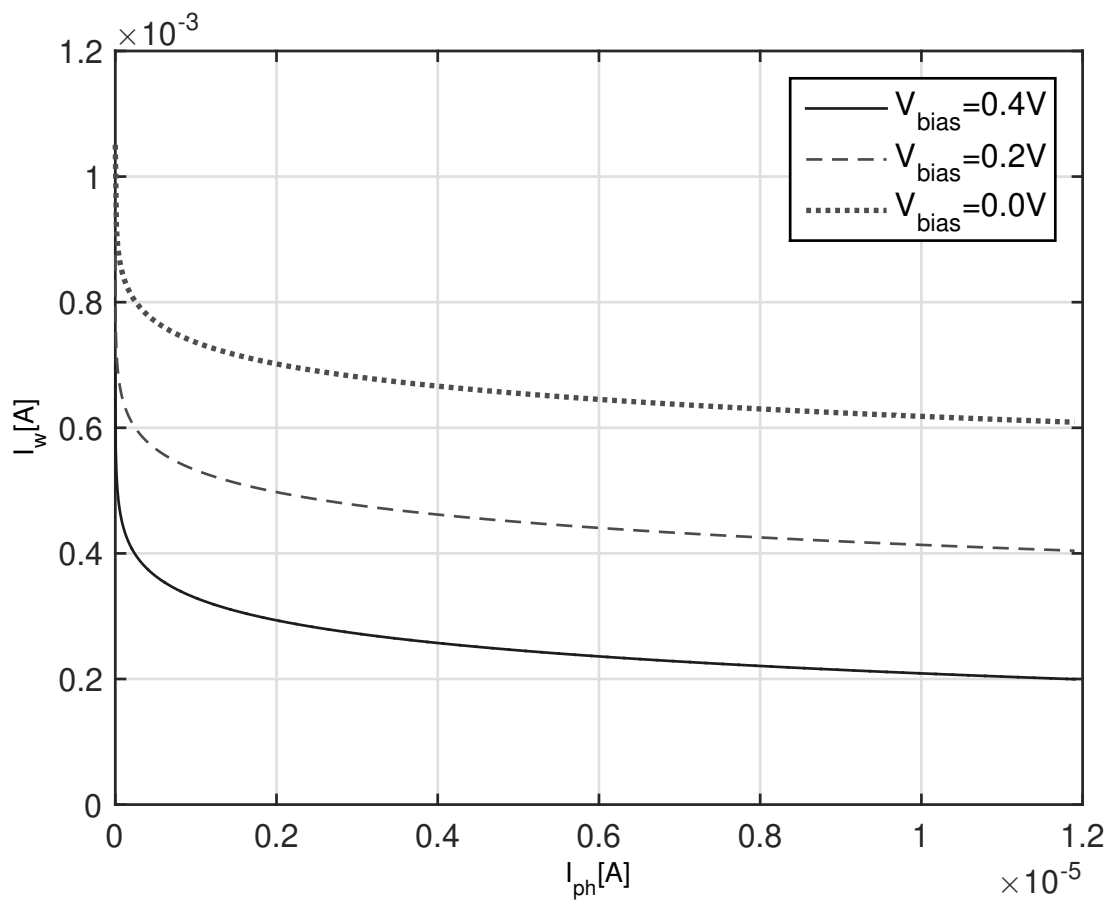


Figure 10: Relationship between the write current at the MTJ device (I_w) and the analog input current (I_{ph}).

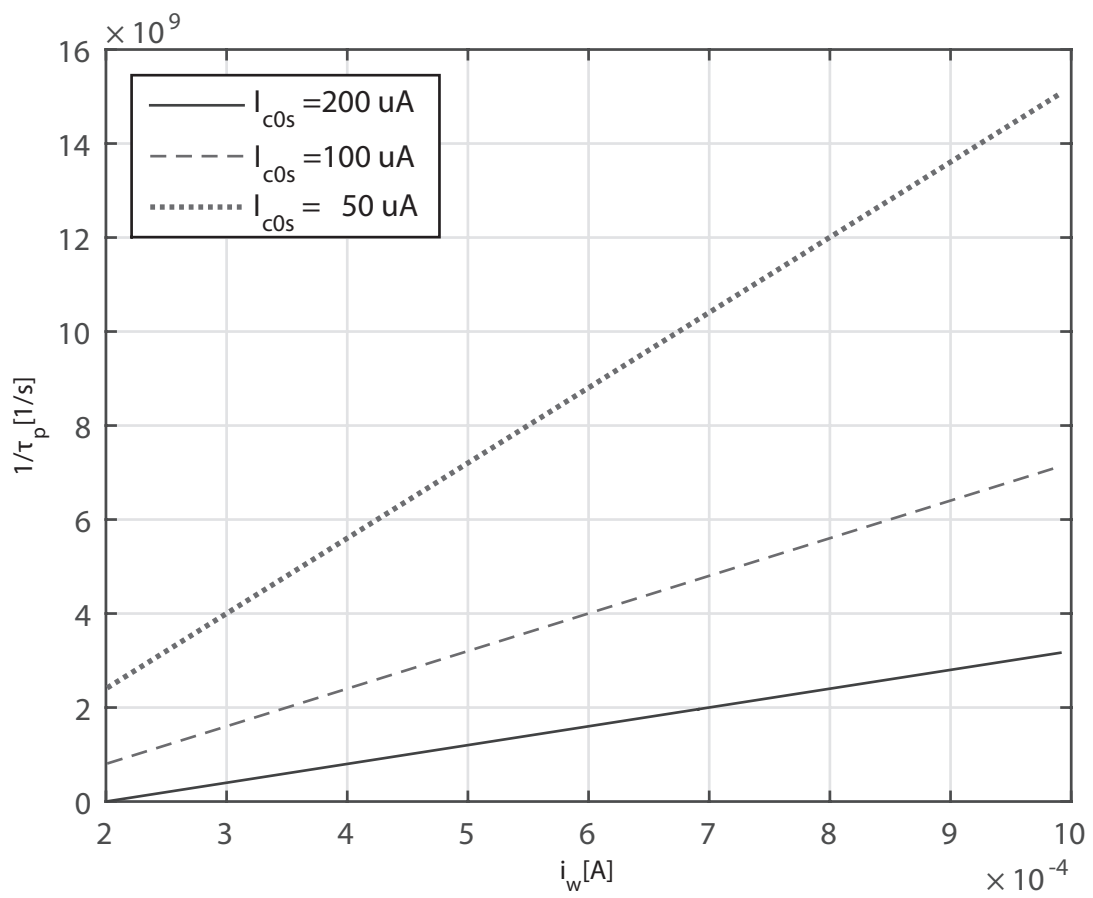


Figure 11: Relationship between inverse of the switching time constant (τ_p) and I_w when V_{bias} is 0.4 V.

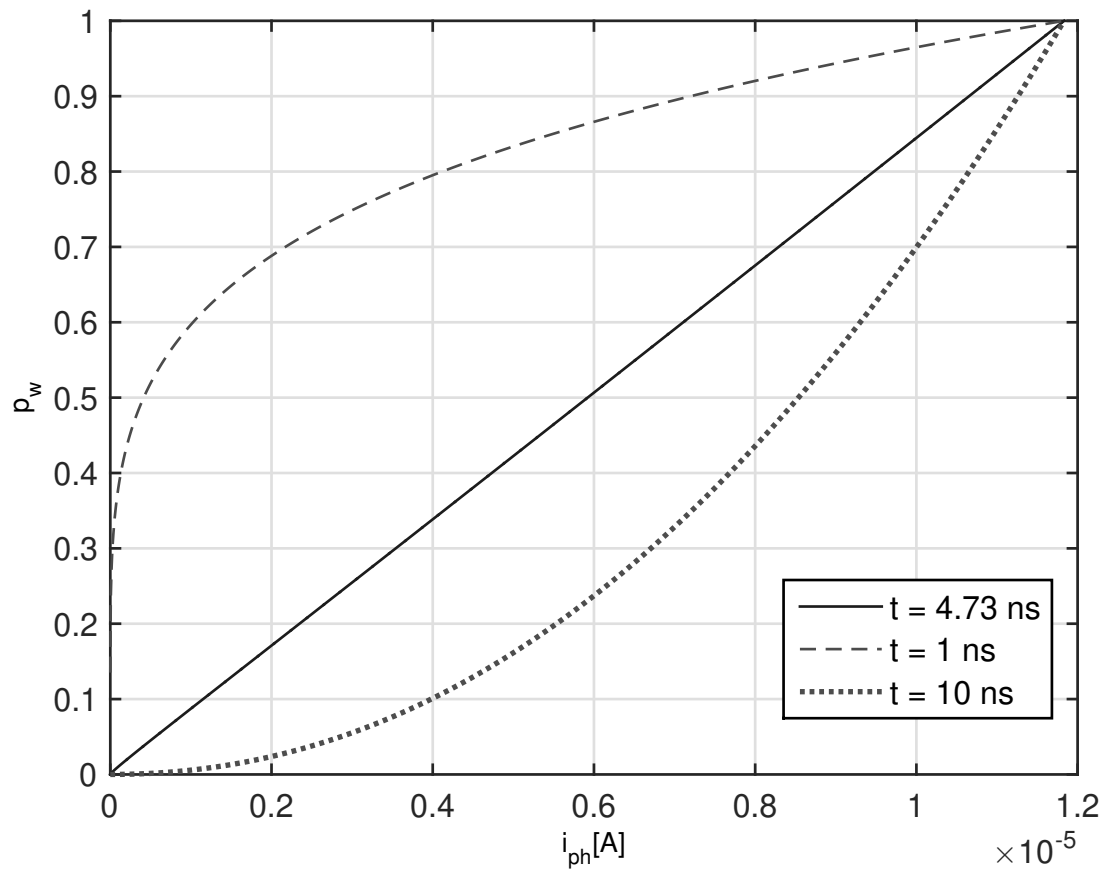


Figure 12: Relationship between the non-switching probability of the MTJ device ($\overline{p_w}$) and i_{ph} when V_{bias} is 0.4 V and I_{c0s} is 200 μ A. The analog-to-stochastic converter is properly designed by setting $t = 4.73$ ns as the linear relationship is realized.

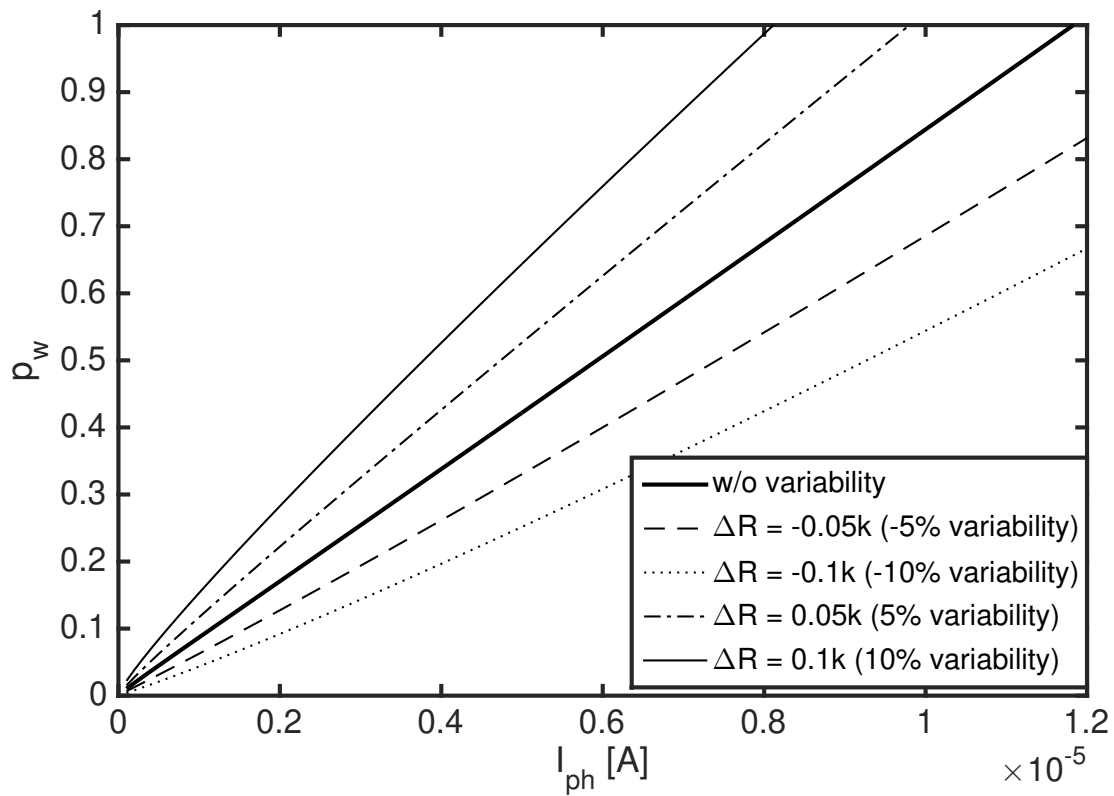


Figure 13: Relationship between the non-switching probability of the MTJ device \bar{p}_w and I_{ph} under the resistance variability of the MTJ device, where V_{bias} is 0.4 V, I_{c0s} is $200 \mu\text{A}$ and t is 4.73 ns.

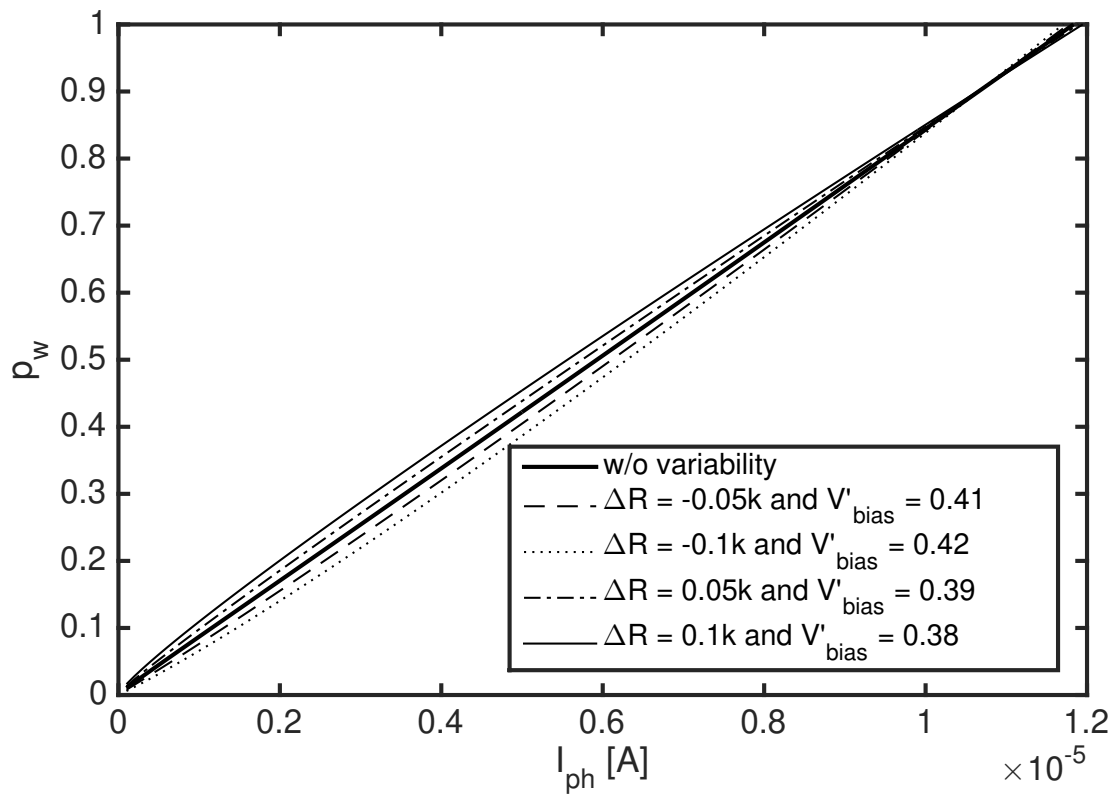


Figure 14: Relationship between the non-switching probability of the MTJ device $\overline{p_w}$ and I_{ph} under the resistance variability, where I_{c0s} is 200 μ A and t is 4.73 ns. The resistance variability is compensated by controlling only V'_{bias} .

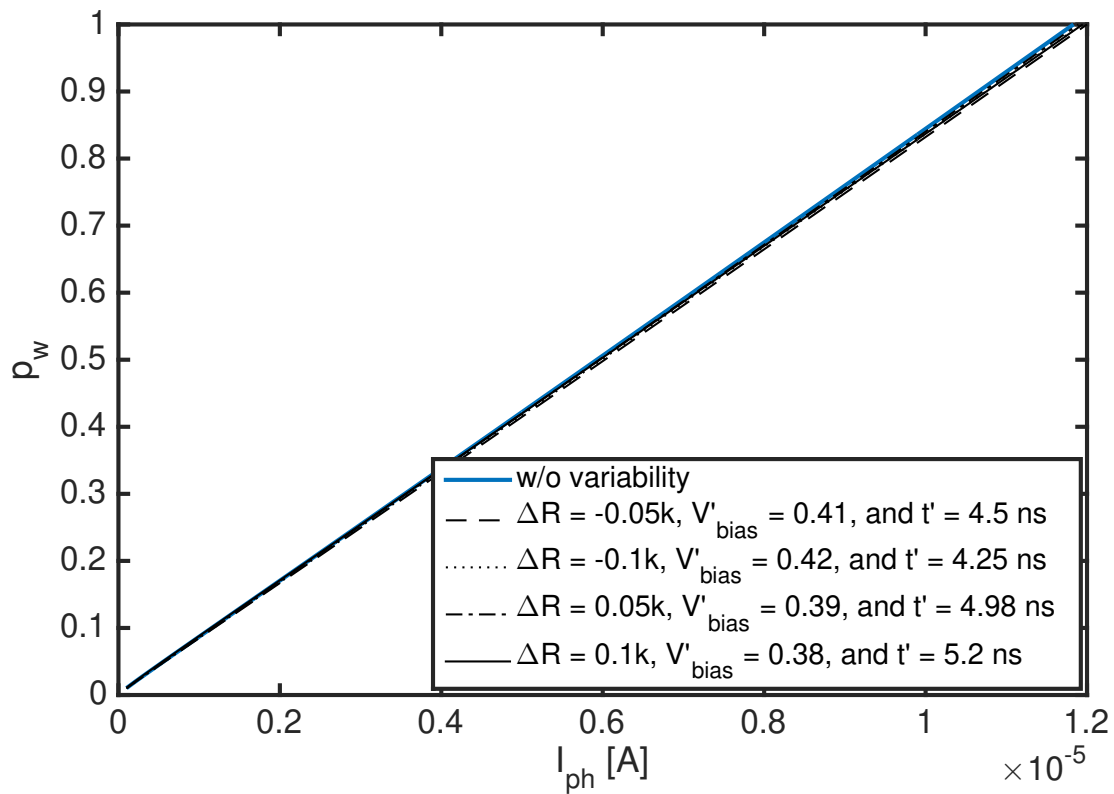


Figure 15: Relationship between the non-switching probability of the MTJ device \bar{p}_w and I_{ph} under the resistance variability where I_{c0s} is $200 \mu\text{A}$. The resistance variability is compensated by controlling V'_bias and t' .

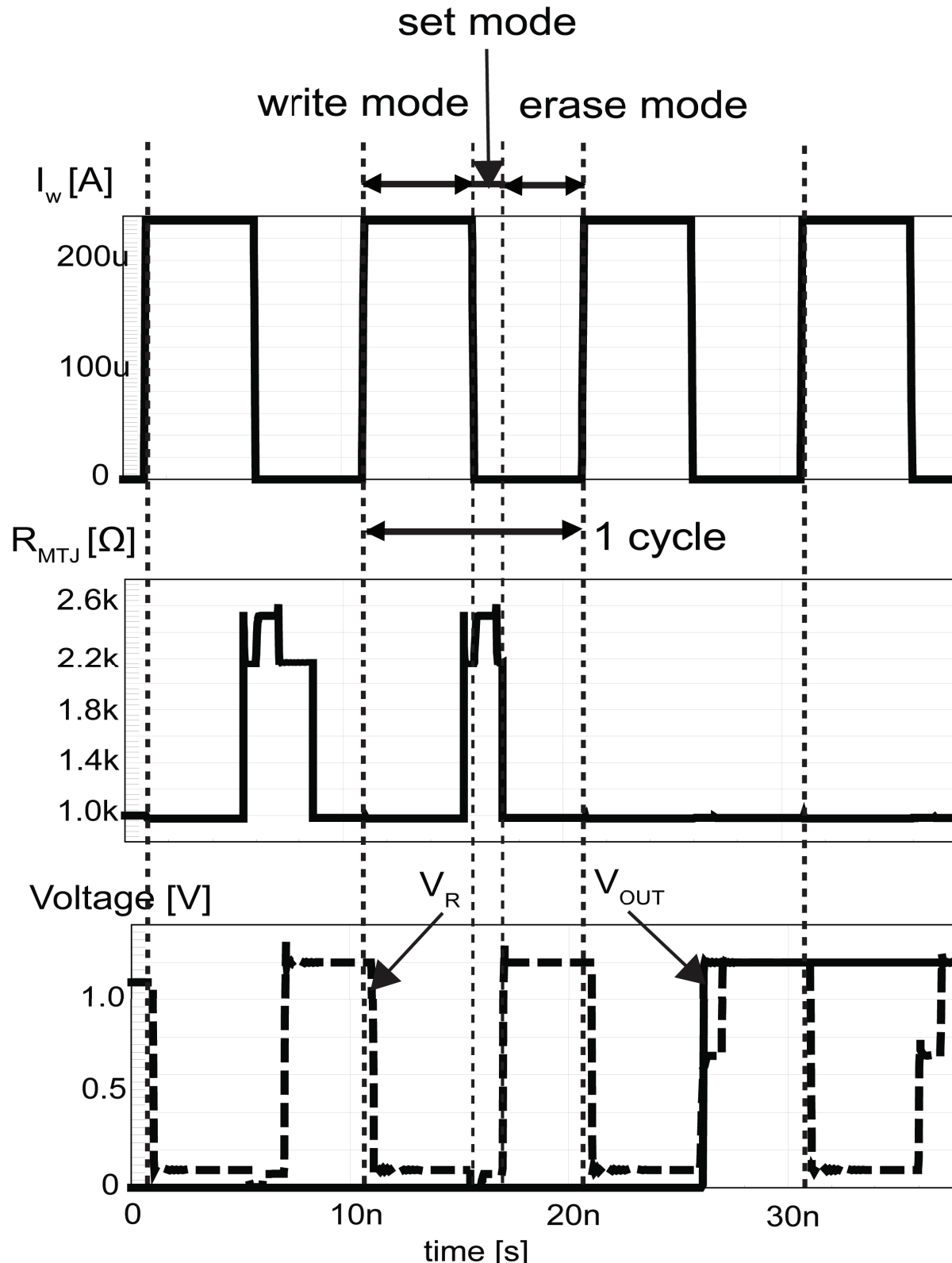


Figure 16: Simulated waveforms of the proposed analog-to-stochastic converter in 90nm CMOS and 100nm MTJ technologies using NS-SPICE. The write current, I_w is 236 μ A corresponding to the switching probability, p_w , of 50%.

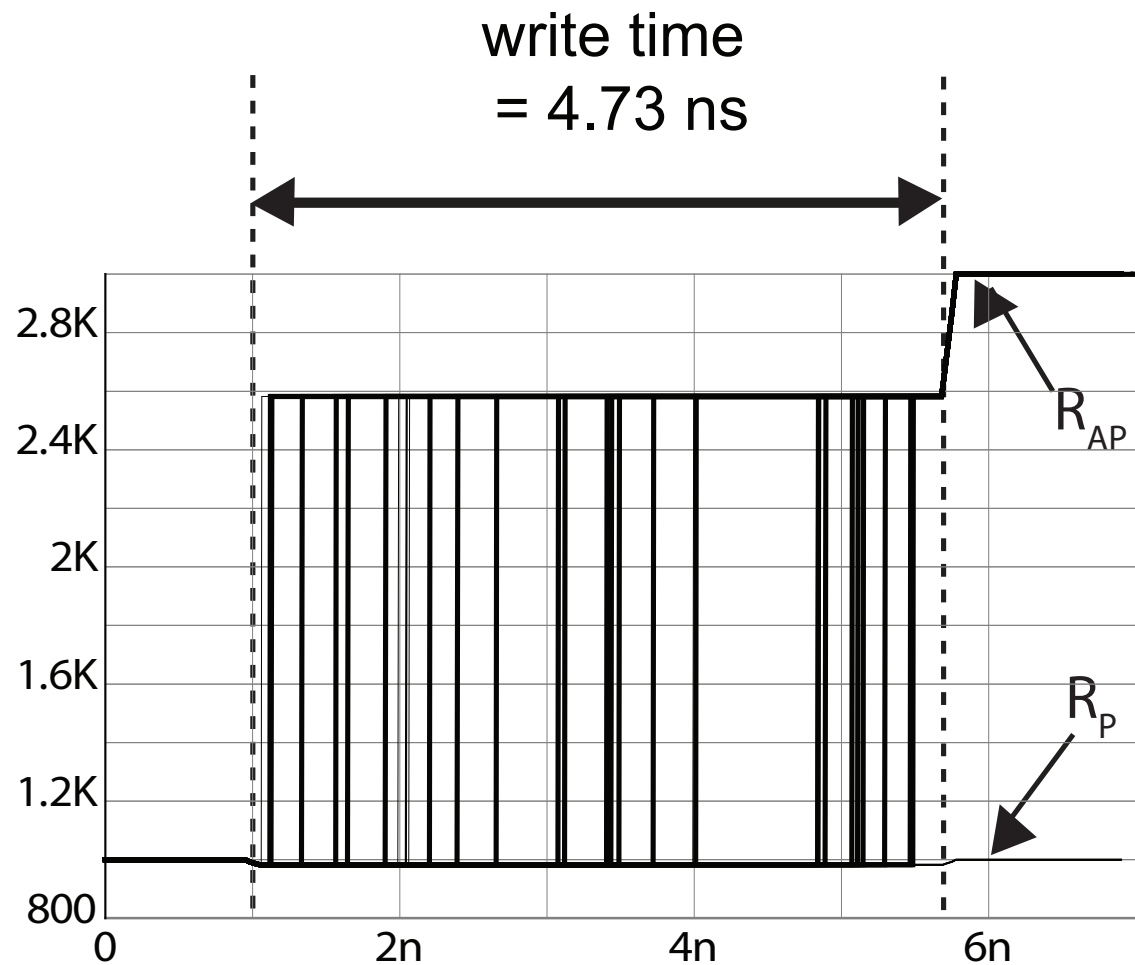


Figure 17: Monte-carlo simulation of the proposed analog-to-stochastic converter, where I_w is $236 \mu\text{A}$ corresponding to $p_W=50\%$ and the number of trials is 100.

Analog-to-Stochastic converter

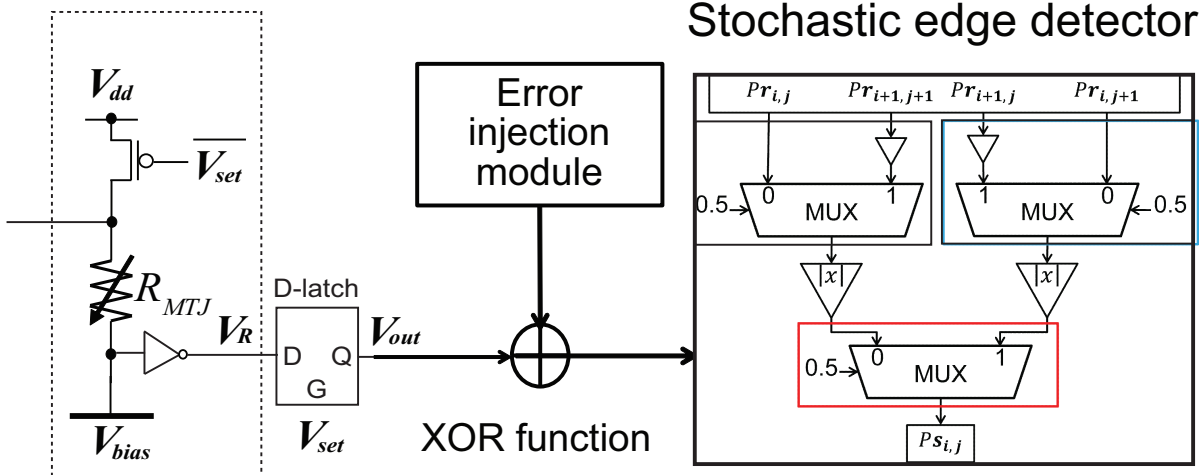


Figure 18: Simulation model of a simple vision chip including an error-injection module in MATLAB.

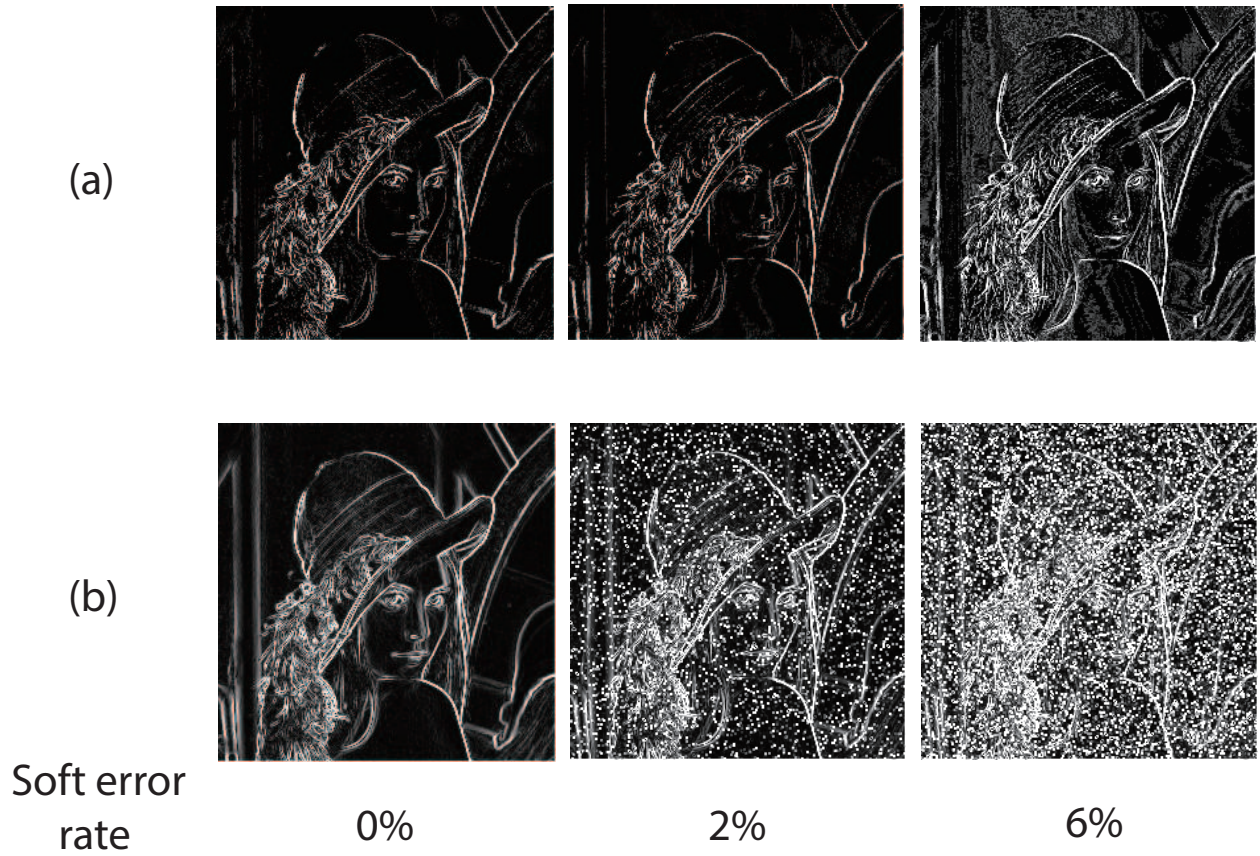


Figure 19: Edge-detection results under input soft errors (a) stochastic implementation and (b) conventional binary implementation.